J. Eng. Technol. Sci., Vol. 54, No. 4, 2022, 220405

Performance Evaluation of a Continuous Downdraft Gasification Reactor Driven by Electric Motors with Manual Mode of Operation

Rachman Setiawan, Hanif Furqon Hidayat, Hafif Dafiqurrohman,
Adi Surjosatyo & Radon Dhelika*

Department of Mechanical Engineering, Faculty of Engineering, Universitas Indonesia,
Kampus UI Depok, 16424, Indonesia
*E-mail: radon@eng.ui.ac.id

Highlights:

- Screw feeder and char removal were tested to analyze how they affect the gasification process.
- A 10-kW biomass gasifier with a circular air intake was tested with various equivalence ratios.
- Evaluation of the 10-kW biomass gasifier showed improved performance and reliability of the gasifier.

Abstract. Gasification is considered a promising option for harnessing energy potential from agricultural waste, such as rice husks. This paper presents a 10-kW rice husk fixed bed gasifier system. This system is an improved version of a prototype previously developed by our research group. Some of the optimized features added to the gasifier include the use of a circular air intake, an improved gas cleaning system, and electric motors that are regulated by a programmable logic controller. Keeping the gasifier system's operation stable is critical for producing high-quality synthetic gas (syngas). Therefore, performance evaluation of the presented gasifier system was conducted, and the resulting syngas outputs were analyzed. The evaluation also included an investigation into the performance of the motors, particularly those used for feeding and char removal, which are critical components of the system. The results showed that the improved gasifier system was stable with a proper feedstock. A discussion of the parameters affecting the composition of the synthetic gas is also presented.

Keywords: *biomass gasification; downdraft fixed bed; motor driver; motor performance; rice husk.*

1 Introduction

Gasification is a chemical process that converts carbon from solid fuel to other forms, such as gas, liquid, or solid. The gasification process is partial oxidation of carbon in a fuel that has gasifying carriers such as oxygen, CO_2, or a flammable gas such as hydrogen [1]. The result of the gasification process is called synthetic

Received August 10th, 2021, December 17th, 2021, Accepted for publication March 24th, 2022.
ISSN: 2337-5779,
DOI: 10.5614/j.eng.technol.sci.2022.54.4.5

gas, or syngas. The main flammable components in syngas are hydrogen (H_2), methane (CH_4), carbon dioxide (CO_2), carbon monoxide (CO), and others in small amounts, such as propane and ethane. Another by-product of gasification is biochar, which contains tar and is composed of an organic fraction that is unconverted and inert material from the biomass [2].

Several processes are involved. First of all, drying is the condition when heat evaporates the moisture of the biomass, which expressed by the following Eq. (1) [3]:

$$r_d = \ 0\, T_s \ < T_{ev} \tag{1}$$

The next stage is pyrolysis, which is divided into two processes, namely tar cracking and primary pyrolysis [4]. The chemical reactions can be written as follows.

In tar cracking:

$$\begin{aligned} Primary\ tar \xrightarrow{r_{p2}} & \ 0.261\ secondary\ tar + 2.6\ CO + 0.441\ CO_2 \\ & +0.983\ CH_4 + 2.161\ H_2 \\ & +0.408\ C_2H_4 \end{aligned} \tag{2}$$

In primary pyrolysis:

$$\begin{aligned} Volatile \xrightarrow{r_{p1}} & \ 0.268\ CO + 0.295\ CO_2 + 0.094\ CH_4 + 0.5\ H_2 + 0.255\ H_2O \\ & +0.004\ NH_3 + 0.002\ H_2S + 0.2\ Primary\ Tar \end{aligned} \tag{3}$$

The third process is oxidation. When the system releases the energy (exotherm) through combustion, the carbon from pyrolysis will react with oxygen, so the carbon will be oxidated to become CO and CO_2, as expressed in Eqs. (4) and (5).

$$C + \frac{1}{2}\, O_2 \rightarrow CO \qquad \Delta H^0_{298} - 110{,}7 \frac{kJ}{mol} \text{ (partial oxidation)} \tag{4}$$

$$C + O_2 \rightarrow CO_2 \qquad \Delta H^0_{298} - 393{,}79 \frac{kJ}{mol} \text{ (fully oxidation)} \tag{5}$$

The last process is reduction, which occurs around 800 to 1000 °C. There are several reactions in this zone: Bouduard reaction, reverse water shift, water-gas reaction, and hydrogasification.

One of the greatest biomass potentials for gasification is rice, which has one of the world's highest biomass potentials. Especially in many Asian countries, rice is the primary staple food for the majority of the population. For every kilogram of harvested paddy rice during harvest, 0.41 to 3.96 kg of straw and 20% to 33% of the weight of paddy rice is rice husk; they are also produced as by-products during the de-husking process [5]. Rice husks have a tremendous energy potential, approximately 15.2-15.3 MJ kg^{-1}, as well as other advantages such as low emission of pollutants (including H_2S, SOx, and NOx) [6]. However, it is necessary to design a gasifier with a medium capacity that is also simple to operate and maintain.

Our group has developed a 10-kW gasifier with rice husks as the feedstock in [7-9]. A downdraft-type of fixed bed design was chosen, because the capacity of this gasifier can range from 10 kW to 1 MW, making it a suitable option for a small-scale system. In addition, gas is produced from the top to the bottom of the reactor, keeping the resulting tar content low (0.015 to 3 g/Nm^3), and is suitable for internal combustion engines. Furthermore, a circular air intake system is used because when air enters the reactor, it must flow from the outer to the inner surface of the reactor, as depicted in Figure 1. The intake air that enters through the primary air must be uniform throughout the partial oxidation zone when pyrolysis occurs by convection. If the process in the pyrolysis zone is not uniform, the decomposition of the rice husk in the pyrolysis process into components such as char, tar, oil, CO, CH_4, and H_2 will be incomplete [10].

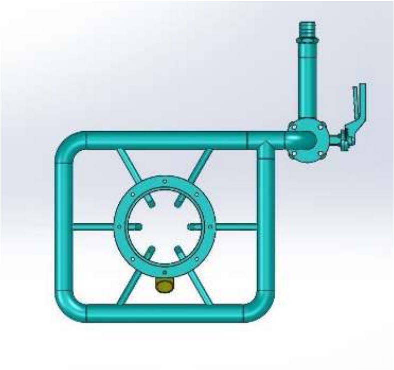

Figure 1 Schematic diagram of circular air intake in the gasifier.

Further consideration must be taken in the design to reduce tar. There are two approaches, i.e., primary and secondary methods. The primary method removes tar in the gasification reactor, whereas the secondary method occurs outside the gasification reactor [11]. However, tar reduction in the primary method cannot meet the requirement of the conversion tool, i.e., a generator engine. Therefore, additional tar removal mechanisms are required to handle tar contained in syngas. In our gasifier system, the secondary method is used by adding a condenser and a filter as the gas cleaning system, which is an optimized component from the previous development [12]. In the previous work, the sustainability of the gasification process was indicated by the related rice husk ash and the feed rate of the biomass feedstock. In this study, an ash disposal modification was introduced to enhance the system, thus increasing the sustainability of the gasification process [13]. A condenser is used to reduce the tar dew point to decrease the tar content in the syngas by converting the phase of the tar from gas to liquid. Filtering is added as a support gas cleaning system, for which rice straw was selected as the filter, since it contains silica that can adsorb tar [14]. Therefore, it is a good material for reducing incondensable tar [15]. In another study, for reducing CO_2 from thermochemical conversions such as gasification, nanofluids were proposed for absorbing CO_2 along with tar removal [16]. Also, for enhanced heat transfer in mixed convection like gasification, a nanofluid could be an optimal option [17,18]. In addition, our gasifier system is also equipped with electric motors to control several actuators. The provision of these motors was expected to improve the operation of the gasifier.

The objective of this work was to evaluate the performance of the 10-kW rice husk fixed bed gasifier. New optimized features added to the gasifier included the use of a circular air intake, an improved gas cleaning system, and motors that are regulated by a programmable logic controller (PLC). The scope of the evaluation included characterization of motor performance, temperature analysis during an experimental run, and evaluation of gas composition.

2 Materials and Methods

2.1 Biomass Feedstock

Rice husk was used in this work as the feedstock to generate syngas. Table 1 shows the ultimate and proximate analyses of the rice husk sample used.

Table 1 Proximate and ultimate analyses of rice husk.

Parameter	Unit	Result	Method
Proximate:			
Moisture in Analysis	%, adb	8.6	ASTM D 3173
Ash Content	%, adb	20.5	ASTM D 3174
Volatile Matter	%, adb	57.6	ISO 562-2010
Fixed Carbon	%, adb	13.3	ASTM D 3172
Ultimate:			
Carbon (C)	%, adb	35.52	ASTM D 5373
Hydrogen (H)	%, adb	5.8	ASTM D 5374
Nitrogen (N)	%, adb	0.5	ASTM D 5375
Oxygen (O)	%, adb	37.6	ASTM D 5376
Sulphur (S)	%, adb	0.12	ASTM D 4239
Higher Heating Value:	kJ/kg	149.182	

2.2 Experimental Setup and P&ID Control

Based on the initial conditions, this experiment used a single-stage process by adding intake air of 4 to 7 Hz that was then converted into an equivalence ratio value. The exhaust blower (EB) as a medium of transferring syngas was regulated at 5 to 15 Hz, with the addition of a vibrating grate (VG) to maintain the continuity of syngas generation in the reactor. The purpose of this experiment was to obtain the optimal operational value to reduce the heating and determine the composition of the resulting syngas. Data were recorded for 15 to 90 min.

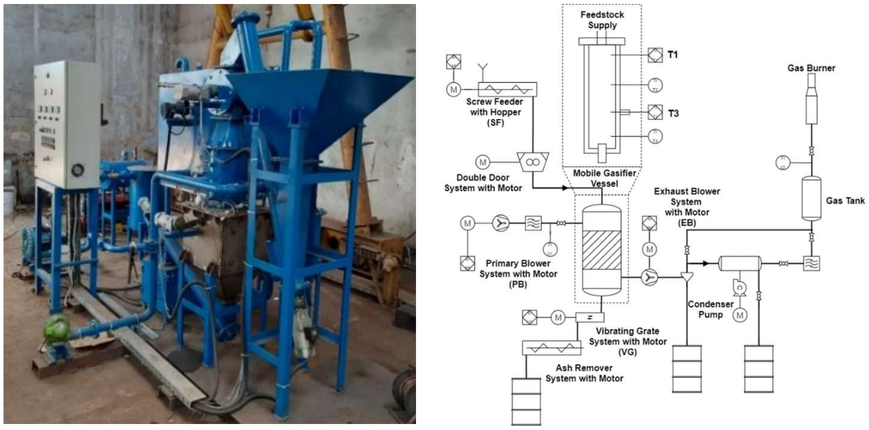

(a) (b)

Figure 2 (a) Experimental and (b) P&ID schematic of the 10-kW downdraft gasifier system used in the experiment.

The general gasification system is depicted in Figure 2(a). The reactor of the gasifier was manufactured from stainless steel SAE 304 with an inner diameter of 254 mm and a height of 600 mm. It was coated with rockwool as an insulator to prevent the heat in the reactor from escaping into the environment. Four thermocouples are attached to the gasification zone (drying, pyrolysis, combustion, and reduction) in the reactor, and two additional thermocouples are attached to the combustion zone and a burner for syngas combustion.

The gasifier has a single air intake that was installed around the reactor to optimize the combustion zone in the gasification process. The feedstock system was made with a screw system with a tilt such that syngas will come out from the reactor through the feedstock channel. The system is also equipped with a rotary blade above the reactor as a syngas barrier at the top of the reactor.

To prevent the reactor from clogging, which will result in a low gas yield, a translational grate system was installed at the bottom of the reactor in the reduction zone through a moving mesh using the SAE 304 material. The system works by converting the rotation of the motor into a two-way motion; after ash falls from the grate, it will be collected by an ash remover system that consists of a screw feeder (SF) and an ash box for storage. The gasification process is closely related to tar reduction. The tar reduction system in this gasifier uses three systems with a cyclone as a separator for solid materials and gas [19], a condenser to reduce tar content through phase changes so that the syngas and the tar can be separated [20], and a filter to absorb tar that cannot be separated in the condenser.

In the tar reduction system, the condenser plays a significant role in the gas cleaning process. Gas that passes through the condenser will drop in temperature and reach the dew point of tar. When the syngas has passed through the condenser, the gas will enter a filter. Tar reduction in the filter uses biomass as the medium; biomass can adsorb tar, and an increase in pressure drop in the syngas flow causes tar to accumulate in the filter [21]. For this gasifier, rice straw and rice husk were selected as filter media because they can be found easily and are suitable for the gasifier feedstock used [22].

The ER values were determined based on the ratio between the actual and the stoichiometric air fuel ratio (AFR), where the sources were obtained from the mass flow from the primary blower, the duration of the experiment, the biomass weight, and the ultimate analysis of the biomass [23] by using Eq. (6) below.

$$ER = \frac{AFR_{actual}}{AFR_{stoichiometri}} \tag{6}$$

Then we use Eqs. (7) and (8) for the actual and the stoichiometric AFR, respectively [24]:

$$AFR_{stoichiometr} = 0.0889\,(\mathrm{C} + 0.375\mathrm{S}) + 0.265\mathrm{H} - 0.0333O \tag{7}$$

$$AFR_{actual} = \frac{\dot{\mathrm{m}}_{air}\ x\ t_{operation}}{m_{fuel}} \tag{8}$$

where the values of C, S, H, and O represent the composition of carbon, sulphur, hydrogen, and oxygen (percent) in the feedstock, $\dot{m}_{air}$ is the total mass flow rate of the incoming air (kg/s), and $t_{operation}$ is the length time of the experiment (seconds).

Four motors are used to actuate the movement of the primary blower (PB), EB, VG (for removing ash in the reactor), and SF. The actuators and their naming are also provided in the P&ID schematic in Figure 2(b). All four actuators are controlled by a variable speed drive. In this research, the load test of SF used an M-6IK200U-SFT motor by Peei Moger with a 1:5 ratio gearbox, while the char removal load test used a Peei Moger M-5IK90U-SF type motor with a 1:5 ratio gearbox. For controlling the motors, a PLC with a manual mode of operation is used; four potentiometers corresponding to the four motors are manually turned by an operator to control actuation. Thus, the PLC will detect the load from the potentiometers and then the controller will set the current for each actuator.

The PLC also provides a safety aspect for the entire system. The panel is equipped with an emergency push button and a thermal magnetic circuit breaker (TMCB). The latter functions as the proponent circuit connecting to the PLC; if any actuator has a fault, the PLC will turn off the system. Both methods have the same frequency range (0 to 50 Hz), and the aim of using a PLC in the system is to maintain the feed rate, ash removal rate, and temperature to make the downdraft gasification system stable and reliable.

In terms of control, a rule-based control mechanism, shown in Table 2, is implemented to operate the gasifier. The rule-based mechanism, comparable to a fuzzy control system, was adapted by modeling a human operator's skill for process control. In addition, it was achieved through structure identification to obtain the best system to operate the actuators [25]. Before regulating the actuators, the operator must monitor the temperature readings in the drying (T1) and combustion (T3) zones because these two parameters serve as essential references for producing synthetic gas. Therefore, regulating these actuators plays an important role in sustainably producing high-quality synthetic gas.

Table 2 Rules in the control system for the gasifier (number in Hz).

T1/T3	**< 80°C**	**80°C–100°C**	**100°C–120°C**	**>120°C**
<400°C	PB = 5	PB = 5	PB = 5	PB = 5
	VG = 0	VG = 0	VG = 0	VG =
	SF = 30	SF = 30	SF = 30	SF = 30
	EB = 5	EB = 7	EB = 7	EB = 7
400°C–600°C	PB = 5	PB = 5	PB = 5	PB = 5
	VG = 7	VG = 8	VG = 8	VG = 8
	SF = 30	SF = 30	SF = 30	SF = 30
	EB = 6	EB = 7	EB = 7	EB = 7
600°C–800°C	PB = 5	PB = 5	PB = 5	PB = 5
	VG = 9	VG = 10	VG = 10	VG = 10
	SF = 30	SF = 30	SF = 30	SF = 30
	EB = 7	EB = 8	EB = 8	EB = 8
>800°C	PB = 5	PB = 5	PB = 5	PB = 5
	VG = 9	VG = 10	VG = 10	VG = 10
	SF = 30	SF = 30	SF = 30	SF = 30
	EB = 9	EB = 9	EB = 9	EB = 9

3 Results and Discussion

3.1 Experimental Set-up and P&ID Control

3.1.1 Screw Feeder Load Test

In this experiment, rice husk was fed to the hopper at the top of the SF with an inclination of 60°. The test was conducted to characterize the performance of the motors. Three parameters were assessed: current, rotational speed, and feed rate. The experiments were run thrice; the average values are plotted in Figure 3.

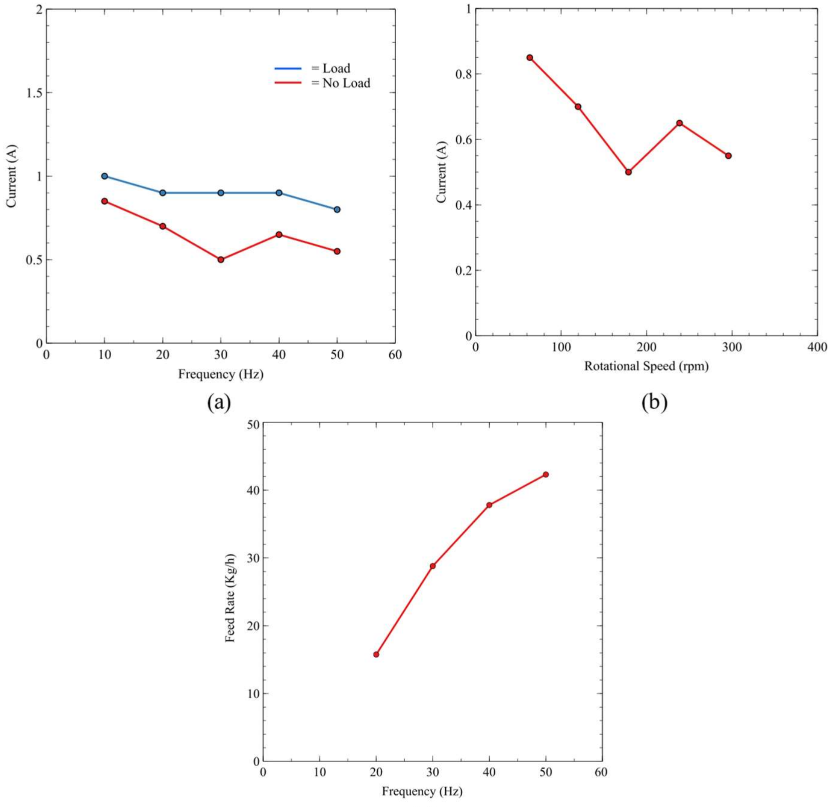

(a)

(b)

(c)

Figure 3 (a) Frequency–current graph in screw feeder test; (b) graph of motor speed to the current in screw feeder; (c) result of feed rate with frequency variation.

Figure 3(a) shows that the load condition draws more current than that without load. It can be surmised that the rice husk load increases torsion in the system, resulting in additional current [26]. In addition, Figure 3(a) shows that the amount of current in the motor was still below the maximum capacity (1.6 A). According to the theory of electric motors, the greater the frequency, the greater the rotational speed. Consequently, the resulting current also decreases. Experimental data obtained, inferred that there was a drop in the current, as shown in Figure 3(b).

In addition, from Figure 3(b), data fluctuations could be observed. This could be due to data floating when the display of the ampere meter was unstable during the measurement, resulting in the captured data being the highest value in the indicator. Furthermore, the feed rate was also obtained by combining the experimental results with the theoretical calculation result shown in Figure 3(c). By obtaining a graph that relates the frequency of the motor to the feed rate, we will be able to control the feeding of rice husk to the reactor by adjusting the frequency of the motor. The calculation of the feed rate was based on theoretical calculations by comparing the design in the first prototype of the gasifier [10], obtained using the following formula using FCR, which is the amount of feedstock per unit time to feed the reactor as formulated below.

$$Fuel\ Consumption\ Rate\ (FCR) = \frac{Qn}{HHV\ x\ \varepsilon g}, \tag{9}$$

where *Qn* represents the energy output value, *HHV* (higher heating value) refers to the calorific value of fuel, and *εg* denotes gasifier efficiency. Based on calculations from Andromeda, *et al*. [7], when the energy output value was 0.01 MW, the calorific value of fuel (HHV) was 15.4 MJ/kg and the gasifier efficiency, including engine efficiency, was 15%, while the theoretical feed rate was 15.58 kg/hour. Figure 3(c) shows that the lowest value generated in the experiment was 13.95 kg/hour. Compared with the theoretical value, the system can exceed the required value. Therefore, the frequency must be set at approximately 20 Hz.

3.1.2 Char Removal Load Test

Char removal is the process of removing the gasification reduction product in the form of ash using a VG. The removed char is then stored in the char storage. A VG mechanism was used to remove char in the reactor; a mesh, coupled by a motor, moves back and forth similar to a piston working mechanism.

The results of the char removal load test are shown in Figures 4(a)-(c). Figure 4(a) shows that there was an increase in current when the load, i.e., rice husk was given to the reactor. However, at a frequency of 10 Hz, the motor experienced a maximum load of 0.7 A, whereas the current limit based on the motor's nameplate is 0.68 A. Therefore, it could be inferred that the VG would become critical when used at low frequencies. The current can exceed the maximum limit because the limit of the TMCB as an electric switch is increased, so the system will increase the temperature in the motor.

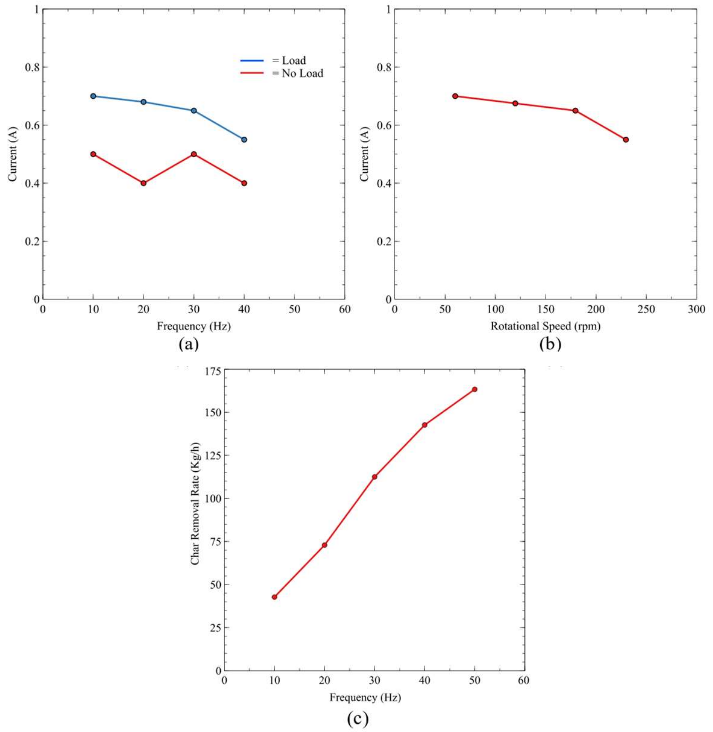

(a)

(b)

(c)

Figure 4 (a) Frequency–current graph for char removal experiment; (b) rotation speed–current graph for char removal test; (c) result of char removal with frequency variation.

The same phenomenon can also be observed in Figure 4(b), where the current decreases with an increase in motor speed. This is comparable to the discussion in the previous section regarding the SF load test. Furthermore, the char removal rate was examined by removing the rice husks at different motor frequencies. This process was preceded by theoretical calculations with the following equation:

$$Char\ Removal\ Rate = FCR * Fuel\ Char\ Mass, \qquad (10)$$

where FCR is the fuel consumption rate. Based on calculations from Andromeda, *et al.* [7], with an FCR of 15.58 kg/hour and a fuel char mass of 18%, the obtained theoretical char removal rate was 2.81 kg/hour. As shown in Figure 4(c), the lowest char removal rate produced in the experiment was 42.75 kg/hour, which exceeded the required limit. On the other hand, the obtained value was too large compared to the required requirements, so the system must be run with an extremely low motor rotation.

3.2 Biomass Gasifier System Analysis

3.2.1 Gasifier Temperature

Four thermocouples were placed in the reactor to record the temperature distribution in real time. The experimental run took approximately 1.5 h from the start to the shutting down of the gasifier. The results are shown in Figure 5. Figure 5(a) depicts the general temperature distribution inside the reactor. The four recorded temperatures represent the different zones of the current process, i.e., drying, pyrolysis, combustion, and reduction. First, the drying process was located 285 mm above the VG, with the temperature reaching approximately 150 °C. Second, the pyrolysis process was approximately 217.50 mm above the VG, with the temperature reaching a range from 200 °C to 350 °C. As shown in Figure 5(a), the temperature rose slightly in the first 35 min and then increased significantly to 300 °C, while the controller was directed by regulators to maintain the temperature at approximately 200 °C. Third, the combustion process was 150 mm above the VG, with the temperature reaching a range of 500 °C to 700 °C.

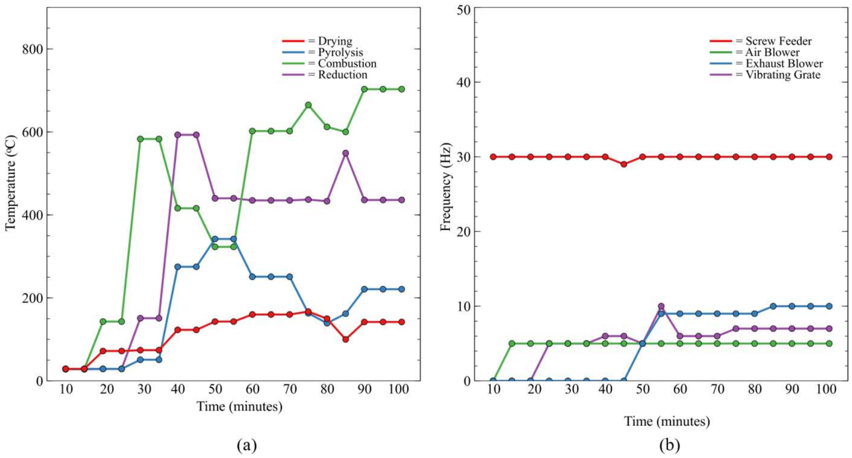

(a) (b)

Figure 5 (a) Temperature in the reactor; (b) regulator performance in controlled actuators.

As depicted in Figure 5(a), the combustion temperature increased drastically at the beginning stage (reaching 583 °C) and then declined gradually because of char removal. Then it increased again, before eventually reaching a steady temperature until the end of the experiment. This increase in temperature was affected by the air fuel intake from the circular tube facing the center of the combustion zone. When the temperature in the combustion zone is high, tar cracking occurs, which improves the calorific and tar value of the gas [22]. Fourth, the reduction process was located at approximately 56 mm above the VG, with a temperature range of 400 °C to 500 °C. At the beginning of the process, as shown in Figure 5(a), a temperature change occurred with a similar value from the combustion to the reduction zone, because the feedstock was being depleted by the VG (char removal started at the 20th minute), so a drastic increase could be observed. However, the decrease in temperature reduced gradually and finally a steady temperature of approximately 450 °C was reached.

To maintain the temperature in the reactor, the four regulators can be controlled manually with potentiometers. The changes in frequency for each motor during the experimental run is shown in Figure 5(b). In this experiment, the system was operated manually. First, the EB was used to transfer the produced syngas to the gas cleaning system. The system was set to run in a frequency range of approximately 5 to 10 Hz to ensure that the gasification process was complete, because if the blower is inclined, the gasification process will be incomplete, which will affect the syngas. Second, the air blower serves to supply fresh air to the reactor through a butterfly valve as safety equipment. For this actuator, the regulator kept a constant level to maintain the ER in the reactor, and this system is supported by an inclined feeder to ensure that there is no additional air supply except from the air blower. Third, the VG functioned to dump char into the screw removal system, and then the char was stored in a box. This system was turned on 32 min after the process began due to a decrease in combustion temperature. However, the gasification process still ran properly until the end of the experiment. The last actuator, the feeder, is used to supply the feedstock to the reactor; the frequency setting was increased by 10 Hz (the standard value based on the load test was 20 Hz) to ensure there was no void in the reactor because rice husk is a low-density matter.

3.2.2 Syngas Composition

The syngas components, which were varied using the ER variable, were CO, H_2, CH_4, and CO_2, as shown in Figure 6(a). Four variations of ER values were set up: 0.23, 0.29, 0.4, and 0.46. The sampling gas was captured after 30 min of experimental run for each variation and was then analyzed by gas chromatography–thermal conductivity detection (an in-house method), which was performed at the Center for Energy Conversion Technology, Agency of

Assessment and Application of Technology. Every experimental run had a typical combination of frequencies for the actuators, but only that of the primary blower was modified to obtain the desired ER.

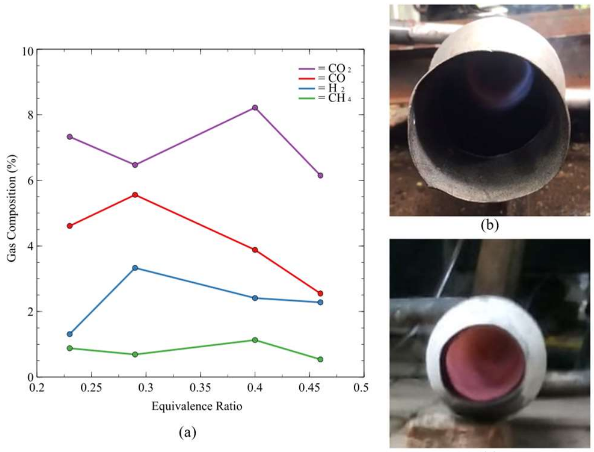

(a)

(b)

(c)

Figure 6 (a) Variation of equivalence ratio (ER) in rice husk gasification, resulting in different syngas compositions; (b) blue flame at ER value of 0.4; (c) red flame in the burner at an ER value of 0.29.

In terms of H_2 concentration, the value was 1.34% when the ER was at 0.23, and it increased gradually to 3.33% when the ER was 0.29. Furthermore, the concentration declined gradually as the ER increased. Similarly, the concentration of CO was 4.62% at an ER of 0.23 and reached its peak at 5.56% before it declined at a high ER. The lowest value of the CO_2 concentration was at an ER of 0.23 when the flammable syngas was the highest. This trend has been similarly reported by Bhoi, *et al.* [25]. On the other hand, the CH_4 content fluctuated, which could be validated by the color of the flame from the burning of the produced syngas. Figure 6(b) shows a blue flame, which corresponds to an ER of 0.4 where the CH_4 content is dominant. Conversely, when the composition of CO was dominant, at an ER value of 0.29, the resulting flame was red, as depicted in Figure 6(c). From Figures 3 (the ability of screw feeder) and 6 (the result of gas composition), it can be seen that the char removal system was successfully implemented to maintain the stability of gasifier operation with the variation of ER that was carried out. However, the char system must be decreased to maximize the syngas generation. If the char system is increased, the syngas will be not totally generated, which influences fully-combusted feedstock in the char storage below the reactor. Moreover, this kind of yield will be injected by an exhaust blower and mixed with the syngas in the burner and constitute bad quality syngas.

From this study, we could obtain the syngas heating value, using an equation obtained from Dafiqurrohman (2016) [10]. It was shown that the highest heating value was reached when the value of ER was 0.29 (1.4 MJ/Kg). However, this value is unusually low due to the design of the reactor (the diameter is too high), which lowers the quality of the syngas. Interestingly, there was a fluctuation trend in CH_4 content at an ER of 0.29, indicated by a red flame. This shows that the gas composition had a majority proportion of CO instead of CH_4, as shown in Figures 6 (a) and (b). In addition, the gasification temperature is also plotted in Figure 7 for different ER variations to validate the process. Figure 7 shows that the gasification temperature increased as the ER increased. This phenomenon was arguably caused by the combustion reaction: products in this zone reacted with oxygen, which resulted in heating due to the oxidation process [26].

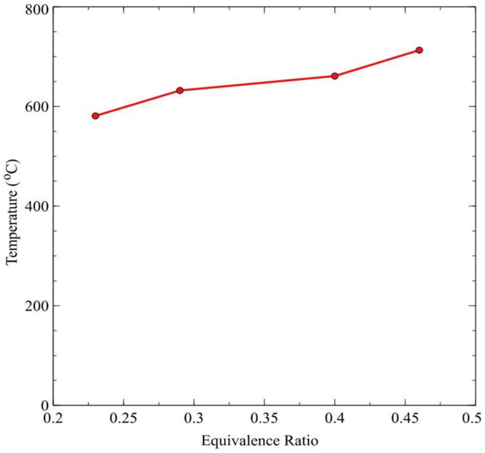

Figure 7 Temperature of the gasifier reactor in terms of varying ER values in gasification of rice husk.

4 Conclusions

In summary, this paper showed the results of a downdraft gasification system that uses rice husk as the feedstock. First, variation of the ER in the downdraft gasifier system affects the composition of the synthetic gas, reactor temperature, and tar content. Furthermore, the best output (syngas) was obtained at an ER of 0.29 in this experiment, when the highest proportions for CO and H_2 were 5.562% and 3.33%, respectively. In addition, the feed rate reached a constant value at 28.8

kg/h or 30 Hz to produce proper syngas with an ER of 0.29 continuously. The results also revealed that the VG for char removal can be stabilized at approximately 5 to 8 Hz to keep the reactor stable with a proper feedstock, so a complete gasification process can be accurately realized. This work hopefully provides insights into the implementation of gasifier systems in real environments, particularly in remote areas, for applications ranging from drying of paddy fields to electricity generation. In the future, the gear system may be improved because a ratio of 1:5 is considered too high for char removal; if the frequency is reduced by approximately 0 to 10 Hz, the current will be high, affecting the temperature of the motor.

Acknowledgment

This work was funded by HIBAH PUTI Q3 fiscal year 2020 (NKB-2013/UN2.RST/HKP.05.00/2020).

References

[1] Basu, P., *Biomass Gasification, Pyrolysis and Torrefaction: Practical Design and Theory*., Ed. 3, Academic Press, 2018.

[2] Molino, A., Chianese, S. & Musmarra, *D., Biomass Gasification Technology: The State-of-the-Art Overview*, J. Energy Chem., **25**(1), pp. 10-25, 2016. DOI: 10.1016/j.jechem.2015.11.005.

[3] Wu, Y., Zhang, Q., Yang, W. & Blasiak, W., *Two-dimensional Computational Fluid Dynamics Simulation of Biomass Gasification in a Downdraft Fixed-Bed Gasifier with Highly Preheated Air and Steam*, Energy and Fuels, **27**(6), pp. 3274-3282, 2013. DOI: 10.1021/ef4003704.

[4] Hejazi, B., Grace, J.R. Bi, X. & Mahecha-Botero, A., *Kinetic Model of Steam Gasification of Biomass in a Bubbling Fluidized Bed Reactor*, Energy and Fuels, **31**(2), pp. 1702-1711, 2017. DOI: 10.1021/acs.energyfuels.6b03161.

[5] Pode, R*., Potential Applications of Rice Husk Ash Waste from Rice Husk Biomass Power Plant*, Renewable and Sustainable Energy Reviews, **53**, pp. 1468-1485, 2016. DOI: 10.1016/j.rser.2015.09.051.

[6] Patel, M. & Karera, A., *Sic Whisker from Rice Husk, Microscopic Study*, Powder Metall. Int., **23**(1), pp. 30-32, 1991.

[7] Andromeda, L., Surjosatyo, A., Dafiqurrohman, H. & Amirullah, M.H., *Analysis of Fix Bed Downdraft Biomass Gasification Reactors Continues Operating Characteristics towards Synthetic Gas Quality*, AIP Conference Proceedings, pp. 030050-1 - 030050-6, 2020. DOI: 10.1063/5.0013681.

[8] Hidayat, H.F., Setiawan, R., Dhelika, R., Surjosatyo, A. & Dafiqurrohman, H., *Investigation of Relative Influence of Process Variables in a 10-Kw*

Downdraft Fixed-Bed Gasifier with Ann Models, J. Appl. Eng. Sci., (Online First), May 26, 2022. DOI: 10.5937/jaes0-34344.

[9] Kurnianto, I.R., Setiawan, A.G., Surjosatyo, A., Dafiqurrohman, H. & Dhelika, R., *Design and Implementation of a Real-Time Monitoring System Based on Internet of Things in a 10-kW Downdraft Gasifier*, Evergreen, **9**(1), pp. 145-149, 2022.

[10] Dafiqurrohman, H., Surjosatyo, A. & Gibran, F.R., *Air Intake Modification for Pyrolysis Optimization on Rice Husk Fixed Bed Downdraft Gasifier with Maximum Capacity of 30 KG/Hour*, Int. J. Technol., **7**(8), pp. 1352-1361, 2016. DOI: 10.14716/ijtech.v7i8.6889.

[11] Yu, H., Zhang, Z., Li, Z. & Chen, D., *Characteristics of Tar Formation during Cellulose, Hemicellulose and Lignin Gasification*, Fuel, **118**, pp. 250-256 2014. DOI: 10.1016/j.fuel.2013.10.080.

[12] Rahman, A.I.M.M., Chowdhury, M.R., Jahan, S. & Uddin, M.R., *Adsorption of Phenol from Aqueous System Using Rice Straw,* Int. J. Eng. Technol, **8**, pp. 841-846, 2011.

[13] Surjosatyo, A., Haq, I., Dafiqurrohman, H. & Gibran, F.R., *Effect of Rice Husk Ash Mass on Sustainability Pyrolysis Zone of Fixed Bed Downdraft Gasifier with Capacity of 10 kg/hour,* AIP Conference Proceedings, pp. 020009-1 - 020009-8, 2017. DOI: 10.1063/1.4979225.

[14] Phuphuakrat, T., Namioka, T. & Yoshikawa, K., *Tar Removal from Biomass Pyrolysis Gas in Two-step Function of Decomposition and Adsorption*, Appl. Energy, **87**(7), pp. 2203-2211, 2010. DOI: 10.1016/j.apenergy.2009.12.002.

[15] Surjosatyo, A., Respati, A., Dafiqurrohman, H. & Muammar*, Analysis of the Influence of Vortexbinder Dimension on Cyclone Separator Performance in Biomass Gasification System,* Procedia Engineering, pp.154-161, 2017. DOI: 10.1016/j.proeng.2017.03.036.

[16] Sodeifian, G. & Niazi, Z., *Prediction of CO_2 Absorption by Nanofluids Using Artificial Neural Network Modeling,* Int. Commun. Heat Mass Transf., **123**, 105193 2021, DOI: 10.1016/j.icheatmasstransfer.2021.105193.

[17] Sepyani, M., Shateri, A. & Bayareh, M., *Investigating the Mixed Convection Heat Transfer of a Nanofluid in a Square Chamber with a Rotating Blade*, J. Therm. Anal. Calorim., **135**, pp. 609-623 2019. DOI: 10.1007/s10973-018-7098-x.

[18] Shirazi, M., Shateri, A. & Bayareh, M., *Numerical Investigation of Mixed Convection Heat Transfer of a Nanofluid in a Circular Enclosure with a Rotating Inner Cylinder*, J. Therm. Anal. Calorim., **133**(2), pp. 1061-1073, 2018. DOI: 10.1007/s10973-018-7186-y.

[19] Dafiqurrohman, H., Bagus Setyawan, M.I., Yoshikawa, K. & Surjosatyo, A., *Tar Reduction Using an Indirect Water Condenser and Rice Straw*

Filter after Biomass Gasification, Case Stud. Therm. Eng., **21**, 100696, 2020. DOI: 10.1016/j.csite.2020.100696.

[20] Thapa, S., Bhoi, P.R., Kumar, A. & Huhnke, R.L., *Effects of Syngas Cooling and Biomass Filter Medium on Tar Removal*, Energies, **10**(3), pp. 349, 2017. DOI: 10.3390/en10030349.

[21] Dafiqurrohman, H., Kosasih, D., Putra, A.W.N., Setyawan, M.I.B. & Surjosatyo, A., *Improvement of Tar Removal Performance in Biomass Gasification Using Fixed-Bed Biomass Filtration*, J. Eng. Technol. Sci., **52**(4), pp. 546-564, 2020. DOI: 10.5614/j.eng.technol.sci.2020.52.4.7.

[22] Bhattacharya, S.C., Shwe Hla, S. & Pham, H.L., *A Study on a Multi-Stage Hybrid Gasifier-Engine System*, Biomass and Bioenergy, **21**(6), pp. 445-460, 2001. DOI: 10.1016/S0961-9534(01)00048-4.

[23] Jain, A.K., *Correlation Models for Predicting Heating Value through Biomass Characteristics*, J. Agric. Eng., **34**(3), pp. 12-25, 1997.

[24] Martínez, J.D., Silva Lora, E.E., Andrade, R.V. & Jaén, R.L., *Experimental Study on Biomass Gasification in a Double Air Stage Downdraft Reactor,* Biomass and Bioenergy, **35**(8), pp. 3465-3480, 2011. DOI: 10.1016/j.biombioe.2011.04.049.

[25] Bhoi, P.R., Huhnke, R.L., Kumar, A., Thapa, S. & Indrawan, N., *Scale-up of a Downdraft Gasifier System for Commercial Scale Mobile Power Generation,* Renew. Energy, **118**, pp. 25-33, 2018. DOI: 10.1016/j.renene.2017.11.002.

[26] Wang, Z., He, T., Qin, J., Wu, J., Li, J., *et al*, *Gasification of Biomass with Oxygen-Enriched Air in a Pilot Scale Two-Stage Gasifier,* Fuel, **150**, pp. 386-393, 2015. DOI: 10.1016/j.fuel.2015.02.056.